View metadata, citation and similar papers at core.ac.uk

brought to you by CORE

provided by Repositório Institucional da Universidade de Aveiro

Author Manuscript

Published in final edited form as:

Composites Part B 154 (2018) 99–107

Doi: 10.1016/j.compositesb.2018.08.001

Title:

Mimicking nature: fabrication of 3D anisotropic electrospun polycaprolactone scaffolds for cartilage tissue engineering applications

*André F. Girão, Ângela Semitela, Gonçalo Ramalho, António Completo and Paula A.A.P. Marques**

TEMA, Department of Mechanical Engineering, University of Aveiro, 3810-193 Aveiro, Portugal.

Corresponding Author: *Paula A.A.P. Marques. Email: paulam@ua.pt

ABSTRACT

There is a growing need to develop strategies capable of engineering the anisotropic cartilaginous fibrous network in vitro and consequently overcome the anatomical and functional restrictions of the standard medical procedures used for cartilage regeneration. In this work, we suggest a fabrication procedure that uses two complementary electrospinning set ups to build 3D multi-layered fibrous scaffolds with adjustable fibre orientation features, matching the topographic cues of the three cartilaginous zones. Polycaprolactone (PCL) was used as bulk material for the different electrospun layers (horizontally, randomly and vertically aligned) that were assembled and then structurally maintained by a biocompatible graphene-oxide-collagen (GO-collagen) microporous network. To validate the resourcefulness of the technique, four PCL-GO-collagen scaffolds with different anisotropic properties were produced and characterized by analysing their depth dependent morphological and mechanical anisotropy. The results confirmed that each electrospun layer presents a similar topography relatively to its natural counterpart and that changing the fibre orientation modifies the compressive behaviour of the scaffold, which is specially influenced by the presence of the vertically aligned fibres. Overall, the presented fabricating technique offers the opportunity to easily tune the anisotropy of 3D electrospun scaffolds towards the enhancement of both static and dynamic cell culture protocols concerning cartilage tissue engineering (TE).

KEYWORDS: Cartilage tissue engineering; Biomimetics; Electrospinning; Anisotropic scaffolds

1. INTRODUCTION

In the human body, each tissue and organ presents a specific composition and architecture responsible for providing biochemical and biophysical cues that ultimately modulate the cell response towards a precise biological function [1]. The partial or total discontinuity of this synergetic pathway due to factors such as aging, disease and/or injury can lead to severe health problems that may not be solved by neither natural regenerative processes nor via standard clinical procedures. Thus, from this perspective, the successfully implementation of TE strategies deeply depends on the ability of the engineered scaffolds to mimic the chemistry and geometry of the injured extracellular matrix (ECM) and consequently trigger the cellular mechanisms that collectively promote regeneration [2]. Biomaterials, especially polymers, are essential components in the biomimetic design of scaffolds since they not only work as bioactive interfaces capable of influencing cell activities like adhesion, proliferation and differentiation, but also offer the possibility to easily engineer composites with advanced 3D architectures [3]. Furthermore, polymers have recently started to be combined with carbon related nanomaterials like graphene and graphene oxide (GO), opening the doors to a new set of composites with enhanced and tunable chemical, electrical, thermal and mechanical properties capable of simulating specific cellular microenvironments [4-5]. Together with the presence of these biocompatible and biologically active composites, the recent successful inclusion of additive manufacturing technologies like electrospinning and 3D printing in biofabrication strategies [6-7] has allowed to narrow the interconnection between function and structure in the next generation of TE scaffolds [8]. In fact, similarly to tissues *in vivo*, a proper geometry is crucial to provide a spatially organized 3D fibrous/porous network capable of promoting *in vitro* cell-scaffold interactions that stimulate the production of new ECM at a ratio compatible with the degradation of the engineered structure [1, 8].

Actually, several studies have already pointed out that the combination of suitable biophysical cues (e.g. chemical, mechanical properties) with 3D geometric features (e.g. porous network and architecture) can lead to a successfully implementation of complementary chemical and morphological gradients [9], to a regulation of cell migration [10] and to a modulation of cell differentiation [11]. For example, in a recent study, Li et al. [12] have reported some advantages of 3D relatively to 2D silk fibroin/chitosan scaffolds, including the ability of the cells to show different morphologies and enhanced migration and differentiation processes.

One of the major challenges of biomimetic designing TE scaffolds is to recreate *in vitro* the hierarchical organization of the fibrous collagen network present in the native cartilage, which is an anisotropic tissue responsible for guaranteeing not only an enhanced load-bearing and load-transferring interface between bones, but also low friction during joint movement [13]. The depth-dependent biomechanical properties of articular cartilage are related with the density and organizational arrangement of its ECM components, particularly the collagen fibrils, which are divided into three functionally complementary nanofibrous zones [14-15]. Indeed, the orientation of the collagen fibres goes from perpendicular to the subchondral bone surface in the deepest zone, to random in the middle zone and finally to parallel in the superficial region. These topographic cues are essential to modulate a suitable cell response because they deeply influence both morphology and function of the chondrocytes and consequently the production and maintenance of the ECM elements. Therefore, the damage of this anisotropic fibrous structure often results in substantial musculoskeletal morbidity since the low proliferative rate and density of chondrocytes together with the avascularity of the cartilaginous tissue do not ensure an appropriate regeneration process [14, 16-17].

In this way, mimicking cartilage requires the design and fabrication of anisotropic scaffolds capable of simulating the hierarchical biochemical, biophysical and geometric depth dependent arrangement of the cartilaginous tissue. Recent studies have reported that advanced hydrogels, including both injectable [18] and stimuli responsive [19], are promising biomimetic platforms for regenerating cartilage since they can guarantee zonal-specific cell responses, for example, by introduction of stiffness gradients [20] or by assembly different layers with specific gelation formulations that consequently ensure particular properties [21]. Additionally, new designs have already overcome some limitations related with the reduced nutrient exchange in the internal regions of tri-layered hydrogels by introducing porous hollow fibres to transport nutrient/waste across the scaffold with the purpose of supporting an optimized and uniform cell behaviour [22]. Alternatively, an enhanced nutrient diffusion in large biocompatible scaffolds can be easily accomplished by 3D printing/bioprinting fabrication [23] due to the possibility to combine the chemical characteristics of bioactive bioinks with accurate mechanical and spatial features [24-26]. Other scaffolding approach involves the development of porous networks that are able to modulate the cell response by adjusting depth dependent architecture gradients related with chemical composition [27] or with pore size [28] and/or orientation [29]. In fact, sequential layers of horizontally, randomly and vertically aligned pores can successfully mimic some structural and biomechanical properties of the superficial, middle and deep zones of the cartilaginous tissue, respectively, leading to an anisotropic scaffold capable of enhancing cellular organization [30]. Moreover, Espinosa et al. [31] have reported that porous scaffolds with chemical and mechanical characteristics similar to native cartilage can spatially control the morphology, orientation and phenotypic state of chondrocytes *in vitro*. However, despite of these promising results, hydrogels and porous scaffolds are not capable of offering biomimetic nanoscale topographic cues analogous to the

fibrous cartilaginous ECM. Hence, scaffolds fabricated by electrospinning are very popular to engineer cartilage since they can easily and cost-effectively produce fibrous meshes with controllable chemical composition, orientation and size [32-33]. Indeed, with the purpose of recreating the geometric characteristics of the cartilaginous tissue, the versatility of electrospinning has allowed the development of multilayer fibrous structures with changes in fibre size and orientation, depending on the parameters used during sequential fibre deposition. For example, McCullen et al. [34] have fabricated trilaminar electrospun scaffolds able to mimic the morphological and functional depth dependent properties of cartilage and consequently enhance a better cell response relatively to homogeneous aligned or random fibrous scaffolds. In other study [35], it was reported a five layered fibrous scaffold capable of not only present an analogous architecture to the cartilage ECM, but also show a depth dependent biological function by sequentially electrospinning two different types of collagen. The hierarchical organization of this scaffold proved to be effective to differentiate Multipotent Mesenchymal Stem Cells into chondrocytes. Although multilayering electrospinning could successfully ensure anisotropic features, the process is time-consuming and the resulting scaffolds usually present low thickness and small pore size. These limitations are incompatible with a functional 3D geometry and therefore, in the last few years, several reports have suggested different methodologies to fabricate 3D electrospun structures [36], including liquid-assisted collection [37], adding sacrificial particles [38] and other alternative strategies [39-40] that sequenced electrospinning, dispersion of nanofibres in liquid and lyophilisation. However these procedures are not able to control the depth dependent variation in fibre orientation, which is a major milestone to engineer a biomimetic cartilaginous microenvironment. Thus, taking all this into account, we purpose a methodology to fabricate 3D electrospun scaffold with distinct biomimetic zones capable of simulating the collagen fibrils anisotropic architecture of the native

cartilage and presenting depth dependent mechanical features. Additionally, the versatility of the technique was also studied by fabricating alternative 3D fibrous geometric architectures that show potential to be used in future static and dynamic cell culture protocols regarding cartilage TE.

2. MATERIALS AND METHODS

2.1. Materials

The PCL with a molecular weight of 80 000 Da, the collagen solution from bovine skin (6 mg mL^{-1}), the Dichloromethane (DMC), the Dimethylformamide (DMF), the Dulbecco's Modified Eagle's Medium/Nutrient Mixture F-12 Ham (DME/F-12, 1:1 mixture), the Penicillin-Streptomycin (Pen-Strep) and the Fetal Bovine Serum (FBS) were purchased from Sigma Aldrich. The GO aqueous dispersion (4.0 mg mL^{-1}, water dispersion) was purchased from Graphenea.

2.2. PCL-GO-collagen scaffolds fabrication

The three fibrous layers (Superficial, Middle and Deep) were fabricated by electrospinning a 12% w/v solution of PCL in a mixture of DCM:DMF with a v:v ratio of 8:2, which was pumped at a controlled a flow rate (1 mL h^{-1}) through a 27-gauge blunt-tip needle with applied voltage of 25 kV. For the superficial and deep layers, the solution was electrospun onto a rotating drum (width = 20 cm; diameter = 20 cm; velocity = 250 RPM) using a working distance of 15 cm. The final thickness of the fibrous mesh was approximately 100 μm. To guarantee the vertical alignment of the deep layer, small rectangles (length = 4 cm; width = 2 mm) were cut from the electrospun mesh and then rolled into spiralled cylinders within a GO-collagen hydrogel, which was fabricated accordingly to our previous work[41]. Briefly, the GO aqueous dispersion was directly mixed with the collagen solution in acidic medium (pH =2) and then rapidly shaken for 10 s in order to form

a hydrogel. The weight % of collagen relatively to GO used was 24. The GO-collagen was then centrifuged (Thermo Scientific™ Heraeus™ Multifuge™ X1 Centrifuge) for 10 minutes at 10 000 RPM with the purpose of removing the excess of water. For the middle layer, an ethanol:water (9:1, v:v) bath was used as a collector with a working distance of 10 cm. The electrospun fibres were collected from the bath after a period of 1.5 minutes of electrospinning.

Previously to the assembly, the three electrospun layers were immersed in water for 5 hours at room temperature. After this period, a cylindrical mould (high = 5 mm; diameter = 5 mm) was used for the assembly: the deep layer was placed into the bottom, followed by the middle layer and then by the superficial layer, which was engineered by pilling up cylinders (high = 100 μm; diameter = 5 mm) cut from the original PCL electrospun mesh. The mould was covered to guarantee the contact between the three fibrous layers and placed at -70°C during a period of 5 hours. The frozen 3D electrospun structure was then removed from the mould and rapidly immersed into the GO-collagen hydrogel placed in a second cylindrical Teflon mould (high = 5 mm; diameter = 10 mm) in order to originate a heterogeneous microporous network after a freeze-drying process at -70°C (Telstar lyoQuest HT-40, Beijer Electronics Products AB) capable of surrounding the fibres and consequently ensuring the correct placement of the assembled layers. The final PCL-GO-collagen scaffold presented a tri-layered structure (geometry 1) and its fabrication is summarized in Figure 1a. Additionally, this methodology was used to fabricate PCL-GO-collagen scaffolds with alternative fibrous geometric architectures by varying the sequence of the different layers during the assembly process (Figure 1b): geometry 2 (superficial + middle layers), geometry 3 (superficial + deep layers) and geometry 4 (middle + deep layers). For these bi-layered PCL-GO-collagen scaffolds, each layer was 2.5 mm high.

2.3. Physicochemical characterization

Chemical analysis of the materials used were performed via attenuated total reflectance Fourier transform infrared (ATR-FTIR) in a Bruker Tensor 27 FT-IR spectrometer (Bruker Corporation). This technique was also used to confirm the success of the self-assembly process of the GO-collagen hydrogel. The spectra were recorded between 4000 and 400 cm^{-1}, with a resolution of 4 cm^{-1} and 256 scans.

The swelling properties of the PCL-GO-collagen scaffolds were determined by immersing the samples into distilled water for 24h at room temperature. The swelling ratio was calculated using 5 specimens of each architecture with the following equation: R = (Ws-Wd)/Wd, where R is the swelling ratio (mg/mg), Ws is the weight of the swollen scaffold and Wd is the weight of the dried scaffold.

2.4. Morphological characterization

The topography features of the three electrospun layers were evaluated individually using a scanning electron microscope (SEM) Hitachi SU 70 (Hitachi High-Technologies) after transversal cuts were made in the PCL-GO-collagen scaffold with the geometry 1. The dimensions of both fibres and pores were evaluated by direct analysis of ten SEM pictures for each sample. These analysis were only made in the PCL-GO-collagen scaffold with the geometry 1 since similar layers (only with different heights) were used for the fabrication of the other geometries.

2.5. Mechanical characterization

The compression properties of the PCL-GO-collagen scaffolds (all geometries) and the three electrospun layers (superficial, middle and deep) were tested by compressing the samples using a Shimadzu MMT-101 N (Shimadzu Scientific Instruments) with a load cell of 100 N. The samples

were compressed at a rate of 1 mm min^{-1} after a pre-charge of 0.07 N and their compressive moduli were calculated by analysing the slope of the stress-strain curves at different strain values (5%, 10%, 15% and 20%). The ratio between compressive moduli at consecutive strains were used as a measure of densification [30]. For each scaffold and layer, 5 specimens were analysed.

The structural integrity of the PCL-GO-collagen scaffolds were studied by submitting one sample of each geometry to a fatigue test inside a bioreactor during 360 hours at 37 °C and 5% CO_2. The samples were immersed in a DME/F-12 + 1% Pen-Strep + 10% FBS medium and submitted to a sinusoidal compression of 10% strain at 0.5 Hz during intervals of 3 h followed by 9 h of rest. The medium was exchanged tree times per week. The Δstress was calculated with the equation: Δstress (Pa) = (σ_{max}-σ_{min}), where σ_{max} and σ_{min} are correspondingly the maximum and minimum stress levels measured during each hour.

3. RESULTS AND DISCUSSION

3.1. Chemical analysis

PCL, GO and collagen were the biomaterials selected for the fabrication of the anisotropic scaffolds since they are very popular in tissue engineering applications due mostly to the manipulation/stability properties [42], functionalization potential [5] and biocompatibility [43], respectively. The ATR-FTIR spectra of these materials are showed in Figure 2, where, as expected, the PCL spectrum (blue) presents its standard absorbance peaks [44] related with the asymmetric CH_2 stretching located at 2958 cm^{-1}, the carbonyl (C=O) stretching at 1724 cm^{-1} and with the asymmetric and symmetric ether (C-O-C) stretching at 1240 cm^{-1} and 1170 cm^{-1}, respectively. On the other hand, the spectrum of the GO-collagen network (black) presents characteristics bands of GO (green) and collagen (red), attesting the success of the self-assembly process between the

negatively charged GO sheets and the positively charged collagen particles in acidic medium [41]. Indeed, it is possible to observe the O-H related peak centred at 3425 cm^{-1} in both GO and GO-collagen spectra. The other GO oxygen moieties can be identified in the peaks located at 1724 cm^{-1} (C=O), 1220 cm^{-1} (C-O epoxy) and 1047 cm^{-1} (C-O alkoxy). In the GO spectrum it is also possible to identify the C=C stretching vibrations at 1623 cm^{-1}. Relatively to collagen, the amide I and III displayed bands can be observed at 1627 cm^{-1} and 1232 cm^{-1}. Additionally, it is also noticeable the characteristic peak of the amide II in both collagen (1540 cm^{-1}) and GO-collagen (at 1535 cm^{-1}) spectra.

3.2. Morphological analysis

As it is shown in Figure 1, it was possible to assemble different fibrous 3D geometries by just varying the combination of the electrospun layers during the assembly process when a mould was used to ensure a proper physical contact between them while freezing. Although this simple process only guarantees a proper integrity of the fibrous structures for a few minutes at room temperature, it was able to preserve their geometries until immersion in the GO-collagen hydrogel before freeze-drying. Then, the final PCL-GO-collagen scaffolds presented their specific fibrous geometries involved and fixed at the centre of a biocompatible GO-collagen microporous network, which presented a pore size distribution suitable for cartilage TE approaches [31, 45] and theoretically capable of guaranteeing an efficient nutrient and oxygen transportation and waste removal into the 3D PCL electrospun structure, where the cells are during the culture periods (Figure 3a). Transversal cuts of the PCL-GO-collagen scaffold with the geometry 1 have confirmed the correct placement of the three electrospun layers and their analogous architecture and topography relatively to their native counterparts. The superficial layer (Figure 3b) presented a network of smooth, defect free electrospun fibres with a diameter of 1.20 ± 0.51 μm. Contrary to other works

that reported highly aligned fibrous systems as superficial regions in anisotropic scaffolds for cartilage TE [34-35], the fabricated electrospun layer shows non-preferential 2D orientation in order to optimize the pore size distribution. In fact, it presents 68 % of pores with diameters between 5 and 10 μm and 16 % of pores with sizes superior to 10 μm. This values could represent an improvement in nutrient diffusion and waste removal across the scaffold and also the enhancement of cell proliferation and migration. For the fabrication of the middle layer (Figure 3c), the PCL was electrospun using an ethanol:water bath as a collector. In this way it was possible to recreate a 3D randomly orientated fibrous network similar to the middle zone of the native cartilage. As expected [46], the electrospun fibres did not present morphological defects and showed a larger fibre diameter (2.00 ± 0.63 μm) and pores with bigger dimensions relatively to the superficial layer, exhibiting 53% of pores between 5 and 10 μm and 31% of pores with a diameter superior to 10 μm. The design and production of this highly porous layer was based on 3D electrospun scaffolds fabricated by wet electrospinning modalities [47-49] that use a liquid with an adequate surface tension as collector to decrease the bulk density of the electrospun mesh and consequently rearrange enhanced (sponge like) fibrous microenvironments that can successfully promote cell infiltration and cartilage matrix formation [50], for example. Finally, the deep layer was engineered by adapting a spiral shaped scaffolding design, which has already prove to be a functional 3D architecture for TE scaffolds since it boosts both the cell infiltration and the nutrient/waste transport across the gaps between the concentric walls, where the cells are attached [51-52]. Indeed, small rectangles were firstly cut from the electrospun mesh and then manually curled into spiralled cylinders with 5 mm of diameter and 2 mm or 2.5 mm of high (depending on the geometry), leading to a fibrous network vertically oriented relative to the superficial layer in a similar fashion of the natural cartilaginous tissue. A analogous approach was already described in other reports, where the electrospun meshes

were rolled up and implanted either with or without cells with the purpose of correcting bone defects *in vivo* [53-54]. For the fabrication of this layer, it was exploited the same electrospun mesh used for the superficial layer since its pores can work as supplementary channels for nutrient diffusion across the spiral branches [55], which would be otherwise only ensured by the longitudinal spaces between them. Actually, in this work, as the rolling process was carried out within a GO-collagen hydrogel, it was possible to guarantee not only the verticality of the electrospun fibres, but also that the same microporous network that surrounds the 3D electrospun system intercalates each fibrous spiral branches after lyophilisation (Figure 3d). Thus, instead of empty spaces, the biocompatible GO-collagen porous arrangement may supply functional bridges between the fibrous walls capable of supporting cells and the newly synthetized ECM. Additionally, the GO-collagen network avoids the compact accumulation of fibres, offering an alternative strategy to other methodologies that involve, for example, the inclusion of microparticles into the electrospun mesh to safeguard an appropriate distance between the fibrous spiral branches [56].

3.3. Mechanical analysis

Taking into account the average deformational behaviour of articular cartilage *in vivo* [14, 57], the mechanical responses under compressive loading of the three electrospun layers used for the fabrication of the different PCL-GO-collagen geometries were studied at low strains ($\varepsilon \leq 20\%$). As it is possible to see in Figure 4a, the three stress-strain curves of the electrospun layers showed linear regimes, indicating that, in all cases, most of the fibres are straight during compression and therefore the following typical events of both fibril [58] and porous [30] systems (buckling, collapsing and densification of the network) were not substantial for the compression regime applied. As expected, the deep layer proved to be significantly more resistant to compression relatively to the superficial and middle layers due to its vertical fibres (Figure 4b). Indeed, the compressive moduli

changed with fibre alignment, decreasing from vertical to random to horizontal. This behaviour matches other reported fibrous and porous anisotropic scaffolds, which resistance to deformation is smaller when the direction of the force is perpendicular to the orientation of the fibres/pores. Relatively to densification of the fibrous networks, it is possible to confirm the interpretation of the stress-strain curves since the values of the compressive moduli ratios are close to 1 (Figure 4c), indicating no considerable changes in the layers architecture. However, it is worthy mention that the ratio of compressive moduli is constantly superior in the superficial layer because of the higher probability of fibre-fibre contact due to its small pores. Thus, it is possible that for higher strains ($\varepsilon > 20\%$) this layer will present more noticeable increasing of resistance during compression relatively to the middle and deep layers, where the larger pore size and the verticality of the fibers could better prevent the contact between fibers. The compressive properties of the electrospun layers are summarized in Table 1.

The combination of these electrospun layers towards the design and fabrication of 3D anisotropic fibrous architectures gave rise to multi-zonal PCL-GO-collagen scaffolds with compressive properties extremely dependent on the geometry used. Predictably, likewise the individual electrospun layers, all the PCL-GO-collagen scaffolds presented linear regimes for the strain interval applied (Figure 5a), indicating the maintenance of their structural and mechanical integrity. The effect of anisotropy is evident by analyzing the compressive moduli in Figure 5b since the values for each scaffold lay between those calculated from the electrospun layers that shape each characteristic geometry. This is particularly noticeable regarding the bi-layered scaffolds because the lowest compressive moduli belongs to the geometry 2, which includes the superficial and middle layers into its fibrous architecture and, on the other hand, the mechanical response of the PCL-GO-collagen scaffold with geometry 4 is the most prominent due to the

combination of the two electrospun layers that better resist compression (middle and deep). Although the influence of the deep layer is also notorious in the compressive response of the scaffold with geometry 3, the horizontal alignment of the fibers in its superficial layer does not provide an efficient resistance to compression. Thus, the PCL-GO-collagen scaffold with this geometry presents an intermediate behavior relatively to geometries 2 and 4. In its turn, the compressive moduli of the tri-layered PCL-GO-collagen scaffold (geometry 1) showed similar values comparatively to the bi-layered PCL-GO-collagen scaffold with geometry 2. This analogous response occurs because the superficial and middle layers represent 60% of the total high of the geometry 1, leading to a more noticeable resistance to compression of these two electrospun layers for low strains. Indeed, the PCL-GO-collagen scaffold with geometry 1 presented ratios of compressive moduli (Figure 5c) that indicate no considerable densification of the 3D structure and therefore no substantial elastic buckling of the vertically aligned fibers of its deep layer. In the same way, the PCL-GO-collagen scaffolds with the other geometries showed densification levels that coincide with their stress-strain curves, meaning no changes in the scaffold architecture induced by compression. All the mechanical testing was performed with swollen samples since water uptake capacity is not only an indispensable requirement to boost cartilage regeneration [39], but also a crucial feature to mimic the physiology of the cartilaginous microenvironment during compression [14]. In fact, besides the physical supporting of the 3D anisotropic structures, an additional advantage of the inclusion of the GO-collagen porous network is to considerably improve the absorbing and retention of water of the scaffolds. In this way, from a functional point a view, it will be possible to both compensate the hydrophobicity and the non-swelling features of PCL, moreover, the swelling ability of the microporous structure guarantees that the PCL-GO-collagen scaffolds return to their original shape after compression. As it is

possible to see from Figure 5d, the swelling ratios of the anisotropic PCL-GO-collagen scaffolds showed comparable values independently of the characteristic geometry used. This is probably due to the PCL nuclei of each scaffold present the same dimensions (5mm of diameter and 5 mm high) and, therefore, a similar proportion of GO-collagen porous network surround them. However, it is possible to observe that the PCL-GO-collagen scaffold with a slightly higher swelling ratio is the one that presents the geometry 4, which it is in accordance with the combination of the larger porous network of the middle layer with a PCL fibrous spiral with branches intercalated with the GO-collagen porous network (deep layer). The compressive and swelling properties of the PCL-GO-collagen scaffold are summarized in Table 2.

There is a wide range of reported Young modulus for the natural cartilage (from 0.1 to 5 MPa) due to not only the complex anatomy and physiology of this anisotropic tissue, but also to its origin and experiment conditions [14, 45, 59]. Taking this into account and considering the value 89.5 ± 48.6 kPa [34] to be the compressive modulus of natural cartilage, the here presented PCL-GO-collagen scaffolds showed a huge potential for cartilage TE applications since their compressive moduli matched this interval, independently of the geometry used. Indeed, these scaffolds offer the opportunity to study how complementary anisotropic 3D fibrous features and, consequently, alternative mechanical properties can affect the cell response towards cartilage regeneration. Specifically, in theory, the different geometries will be able to induce singular depth dependent cellular densities, orientations and morphologies that could lead to dissimilar localized ECM production elements [31, 34-35, 60-61] and subsequently to alternative cellular platforms that might be selected depending on the specific requirements of the followed TE strategy. Additionally, the inclusion of *in vitro* mechanical stimulation provided by bioreactors in such TE approaches is a growing modality since cells can sense and transform external mechanical stimuli into biochemical

signalling pathways that can decisively impact cellular events such as ECM production and cell differentiation [62-64]. In this regard, the viability of PCL-GO-collagen scaffolds to integrate dynamic mechanical stimulation protocols was evaluated within a patented bioreactor apparatus [65] (Figure 6a) capable of providing a controlled uniaxial mechanical loading strain and frequency. As it is possible to see from Figure 6b, the scaffolds were able to maintain their mechanical integrity after 360 hours of testing, as it is revealed by the constant value of Δstress measured for the intercalated stimulation periods (8.21 ± 0.50 kPa). This result, although preliminary, is an excellent indicator for the ability of these scaffolds to positively respond to induced mechanical loading, leading to a wider range of promising cell culture conditions that can be combined towards an optimized cartilage regeneration.

4. CONCLUSION

In this study, we developed a viable methodology to fabricate functional 3D anisotropic electrospun scaffolds with customized fibrous geometries for cartilage TE applications. Indeed, by using two complementary electrospinning set ups, it was possible to engineer layers with fiber orientation and mechanical properties that were similar to their cartilaginous counterparts. Such layers were then assembled into distinct 3D scaffolds with alternative depth dependent topographic and mechanical properties, depending on the geometry applied. Therefore, the versatility of the presented fabrication technique allows the recreation of suitable platforms able to match the specifications of each particular experiment, including both static and dynamic cell culture protocols regarding cartilage TE.

ACKNOWLEDGMENTS

This work was supported by the funding of Program COMPETE-FEDER, Programa Operacional Competitividade e Internacionalização through the project POCI-01-0145-FEDER-016574 and by Fundação para a Ciencia e Tecologia I.P. (FCT, IP) through the project PTDC/EMS-TEC/3263/2014 and IF/00917/2013/CP1162/CT0016. The authors thank to FCT for the PhD grants SFRH/BD/130287/2017 and SFRH/BD/133129/2017. The authors are also grateful for the generosity and valuable input of Ana João Nóbrega, Sofia S. Almeida and Susana Cristina.

REFERENCES

(1) Li, Y.; Xiao, Y.; Liu, C. The Horizon of Materiobiology: A Perspective on Material-Guided Cell Behaviors and Tissue Engineering. *Chem. Rev.* **2017,** *117* (5), 4376-4421, DOI: 10.1021/acs.chemrev.6b00654.

(2) Khademhosseini, A.; Langer, R. A decade of progress in tissue engineering. *Nat. Protoc.* **2016,** *11*, 1775, DOI: 10.1038/nprot.2016.123.

(3) Ratheesh, G.; Venugopal, J. R.; Chinappan, A.; Ezhilarasu, H.; Sadiq, A.; Ramakrishna, S. 3D Fabrication of Polymeric Scaffolds for Regenerative Therapy. *ACS Biomater Sci Eng* **2017,** *3* (7), 1175-1194, DOI: 10.1021/acsbiomaterials.6b00370.

(4) Shin, S. R.; Li, Y.-C.; Jang, H. L.; Khoshakhlagh, P.; Akbari, M.; Nasajpour, A.; Zhang, Y. S.; Tamayol, A.; Khademhosseini, A. Graphene-based materials for tissue engineering. *Adv. Drug Del. Rev.* **2016,** *105*, 255-274, DOI: https://doi.org/10.1016/j.addr.2016.03.007.

(5) Ege, D.; Kamali, A. R.; Boccaccini, A. R. Graphene Oxide/Polymer-Based Biomaterials. *Adv. Eng. Mater.* **2017,** *19* (12), 1700627, DOI: 10.1002/adem.201700627.

(6) Moroni, L.; Boland, T.; Burdick, J. A.; De Maria, C.; Derby, B.; Forgacs, G.; Groll, J.; Li, Q.; Malda, J.; Mironov, V. A.; Mota, C.; Nakamura, M.; Shu, W.; Takeuchi, S.; Woodfield, T. B. F.; Xu, T.; Yoo, J. J.; Vozzi, G. Biofabrication: A Guide to Technology and Terminology. *Trends Biotechnol.* **2017**, DOI: https://doi.org/10.1016/j.tibtech.2017.10.015.

(7) Dutta, R. C.; Dey, M.; Dutta, A. K.; Basu, B. Competent processing techniques for scaffolds in tissue engineering. *Biotechnol Adv* **2017,** *35* (2), 240-250, DOI: 10.1016/j.biotechadv.2017.01.001.

(8) Mansouri, N.; SamiraBagheri. The influence of topography on tissue engineering perspective. *Mater Sci Eng C Mater Biol Appl* **2016,** *61*, 906-21, DOI: 10.1016/j.msec.2015.12.094.

(9) D'Amora, U.; D'Este, M.; Eglin, D.; Safari, F.; Sprecher, C. M.; Gloria, A.; De Santis, R.; Alini, M.; Ambrosio, L. Collagen density gradient on three-dimensional printed poly(ε-caprolactone) scaffolds for interface tissue engineering. *J Tissue Eng Regen Med* **2017**, 1-9, DOI: 10.1002/term.2457.

(10) Caballero, D.; Palacios, L.; Freitas, P. P.; Samitier, J. An Interplay between Matrix Anisotropy and Actomyosin Contractility Regulates 3D-Directed Cell Migration. *Adv. Funct. Mater.* **2017,** *27* (35), 1702322, DOI: 10.1002/adfm.201702322.

(11) Zujur, D.; Kanke, K.; Lichtler, A. C.; Hojo, H.; Chung, U.-i.; Ohba, S. Three-dimensional system enabling the maintenance and directed differentiation of pluripotent stem cells under defined conditions. *Sci. Adv.* **2017,** *3* (5).

(12) Li, D.-W.; He, F.-L.; He, J.; Deng, X.; Liu, Y.-L.; Liu, Y.-Y.; Ye, Y.-J.; Yin, D.-C. From 2D to 3D: The morphology, proliferation and differentiation of MC3T3-E1 on silk fibroin/chitosan matrices. *Carbohydr. Polym.* **2017,** *178*, 69-77, DOI: https://doi.org/10.1016/j.carbpol.2017.09.035.

(13) Armiento, A. R.; Stoddart, M. J.; Alini, M.; Eglin, D. Biomaterials for articular cartilage tissue engineering: Learning from biology. *Acta Biomater.* **2018,** *65*, 1-20, DOI: https://doi.org/10.1016/j.actbio.2017.11.021.

(14) Camarero-Espinosa, S.; Rothen-Rutishauser, B.; Foster, E. J.; Weder, C. Articular cartilage: from formation to tissue engineering. *Biomater Sci* **2016,** *4* (5), 734-767, DOI: 10.1039/c6bm00068a.

(15) Sophia Fox, A. J.; Bedi, A.; Rodeo, S. A. The Basic Science of Articular Cartilage: Structure, Composition, and Function. *Sports Health* **2009,** *1* (6), 461-468, DOI: 10.1177/1941738109350438.

(16) Grogan, S. P.; Duffy, S. F.; Pauli, C.; Koziol, J. A.; Su, A. I.; D'Lima, D. D.; Lotz, M. K. Zone-specific Gene Expression Patterns in Articular Cartilage. *Arthritis and rheumatism* **2013,** *65* (2), 418-428, DOI: 10.1002/art.37760.

(17) Hunziker, E. B.; Lippuner, K.; Keel, M. J. B.; Shintani, N. An educational review of cartilage repair: precepts & practice – myths & misconceptions – progress & prospects. *Osteoarthr. Cartil.* **2015,** *23* (3), 334-350, DOI: https://doi.org/10.1016/j.joca.2014.12.011.

(18) Liu, M.; Zeng, X.; Ma, C.; Yi, H.; Ali, Z.; Mou, X.; Li, S.; Deng, Y.; He, N. Injectable hydrogels for cartilage and bone tissue engineering. *Bone Res* **2017,** *5*, 17014, DOI: 10.1038/boneres.2017.14.

(19) Eslahi, N.; Abdorahim, M.; Simchi, A. Smart Polymeric Hydrogels for Cartilage Tissue Engineering: A Review on the Chemistry and Biological Functions. *Biomacromolecules* **2016,** *17* (11), 3441-3463, DOI: 10.1021/acs.biomac.6b01235.

(20) Zhu, D.; Tong, X.; Trinh, P.; Yang, F. Mimicking Cartilage Tissue Zonal Organization by Engineering Tissue-Scale Gradient Hydrogels as 3D Cell Niche. *Tissue Eng Part A* **2018,** *24* (1-2), 1-10, DOI: 10.1089/ten.TEA.2016.0453.

(21) Walker, K. J.; Madihally, S. V. Anisotropic temperature sensitive chitosan-based injectable hydrogels mimicking cartilage matrix. *J. Biomed. Mater. Res. B* **2015,** *103* (6), 1149-1160, DOI: 10.1002/jbm.b.33293.

(22) Kim, M.; Farrell, M. J.; Steinberg, D. R.; Burdick, J. A.; Mauck, R. L. Enhanced nutrient transport improves the depth-dependent properties of tri-layered engineered cartilage constructs with zonal co-culture of chondrocytes and MSCs. *Acta Biomater.* **2017,** *58*, 1-11, DOI: https://doi.org/10.1016/j.actbio.2017.06.025.

(23) O'Connell, G.; Garcia, J.; Amir, J. 3D Bioprinting: New Directions in Articular Cartilage Tissue Engineering. *ACS Biomater Sci Eng* **2017,** *3* (11), 2657-2668, DOI: 10.1021/acsbiomaterials.6b00587.

(24) Park, J. Y.; Choi, Y.-J.; Shim, J.-H.; Park, J. H.; Cho, D.-W. Development of a 3D cell printed structure as an alternative to autologs cartilage for auricular reconstruction. *J. Biomed. Mater. Res. B* **2017,** *105* (5), 1016-1028, DOI: 10.1002/jbm.b.33639.

(25) Zhou, X.; Nowicki, M.; Cui, H.; Zhu, W.; Fang, X.; Miao, S.; Lee, S.-J.; Keidar, M.; Zhang, L. G. 3D bioprinted graphene oxide-incorporated matrix for promoting chondrogenic differentiation of human bone marrow mesenchymal stem cells. *Carbon* **2017,** *116*, 615-624, DOI: https://doi.org/10.1016/j.carbon.2017.02.049.

(26) Yang, X.; Lu, Z.; Wu, H.; Li, W.; Zheng, L.; Zhao, J. Collagen-alginate as bioink for three-dimensional (3D) cell printing based cartilage tissue engineering. *Materials Science and Engineering: C* **2018,** *83*, 195-201, DOI: https://doi.org/10.1016/j.msec.2017.09.002.

(27) Zhu, Y.; Wan, Y.; Zhang, J.; Yin, D.; Cheng, W. Manufacture of layered collagen/chitosan-polycaprolactone scaffolds with biomimetic microarchitecture. *Colloids Surf. B. Biointerfaces* **2014,** *113*, 352-360, DOI: https://doi.org/10.1016/j.colsurfb.2013.09.028.

(28) Zhang, Q.; Lu, H.; Kawazoe, N.; Chen, G. Pore size effect of collagen scaffolds on cartilage regeneration. *Acta Biomater.* **2014,** *10* (5), 2005-2013, DOI: https://doi.org/10.1016/j.actbio.2013.12.042.

(29) Zhang, Y.; Ye, L.; Cui, J.; Yang, B.; Sun, H.; Li, J.; Yao, F. A Biomimetic Poly(vinyl alcohol)–Carrageenan Composite Scaffold with Oriented Microarchitecture. *ACS Biomater Sci Eng* **2016,** *2* (4), 544-557, DOI: 10.1021/acsbiomaterials.5b00535.

(30) Arora, A.; Kothari, A.; Katti, D. S. Pore orientation mediated control of mechanical behavior of scaffolds and its application in cartilage-mimetic scaffold design. *J Mech Behav Biomed Mater* **2015,** *51*, 169-183, DOI: https://doi.org/10.1016/j.jmbbm.2015.06.033.

(31) Camarero-Espinosa, S.; Rothen-Rutishauser, B.; Weder, C.; Foster, E. J. Directed cell growth in multi-zonal scaffolds for cartilage tissue engineering. *Biomaterials* **2016,** *74*, 42-52, DOI: https://doi.org/10.1016/j.biomaterials.2015.09.033.

(32) Khorshidi, S.; Solouk, A.; Mirzadeh, H.; Mazinani, S.; Lagaron, J. M.; Sharifi, S.; Ramakrishna, S. A review of key challenges of electrospun scaffolds for tissue-engineering applications. *J Tissue Eng Regen Med* **2016,** *10* (9), 715-738, DOI: 10.1002/term.1978.

(33) M, J. C.; Reardon, P. J. T.; Konwarh, R.; Knowles, J. C.; Mandal, B. B. Mimicking Hierarchical Complexity of the Osteochondral Interface Using Electrospun Silk–Bioactive Glass Composites. *ACS Appl. Mater. Interfaces* **2017,** *9* (9), 8000-8013, DOI: 10.1021/acsami.6b16590.

(34) McCullen, S. D.; Autefage, H.; Callanan, A.; Gentleman, E.; Stevens, M. M. Anisotropic Fibrous Scaffolds for Articular Cartilage Regeneration. *Tissue Engineering. Part A* **2012,** *18* (19-20), 2073-2083, DOI: 10.1089/ten.tea.2011.0606.

(35) Reboredo, J. W.; Weigel, T.; Steinert, A.; Rackwitz, L.; Rudert, M.; Walles, H. Investigation of Migration and Differentiation of Human Mesenchymal Stem Cells on Five-Layered Collagenous Electrospun Scaffold Mimicking Native Cartilage Structure. *Adv Healthc Mater* **2016,** *5* (17), 2191-2198, DOI: 10.1002/adhm.201600134.

(36) Sun, B.; Long, Y. Z.; Zhang, H. D.; Li, M. M.; Duvail, J. L.; Jiang, X. Y.; Yin, H. L. Advances in three-dimensional nanofibrous macrostructures via electrospinning. *Prog. Polym. Sci.* **2014,** *39* (5), 862-890, DOI: https://doi.org/10.1016/j.progpolymsci.2013.06.002.

(37) Zheng, X.; Wang, W.; Liu, S.; Wu, J.; Li, F.; Cao, L.; Liu, X.-d.; Mo, X.; Fan, C. Enhancement of chondrogenic differentiation of rabbit mesenchymal stem cells by oriented nanofiber yarn-collagen type I/hyaluronate hybrid. *Materials Science and Engineering: C* **2016,** *58*, 1071-1076, DOI: https://doi.org/10.1016/j.msec.2015.07.066.

(38) Lavielle, N.; Hébraud, A.; Schlatter, G.; Thöny-Meyer, L.; Rossi, R. M.; Popa, A.-M. Simultaneous Electrospinning and Electrospraying: A Straightforward Approach for Fabricating Hierarchically Structured Composite Membranes. *ACS Appl. Mater. Interfaces* **2013,** *5* (20), 10090-10097, DOI: 10.1021/am402676m.

(39) Chen, W.; Chen, S.; Morsi, Y.; El-Hamshary, H.; El-Newhy, M.; Fan, C.; Mo, X. Superabsorbent 3D Scaffold Based on Electrospun Nanofibers for Cartilage Tissue Engineering. *ACS Appl. Mater. Interfaces* **2016,** *8* (37), 24415-24425, DOI: 10.1021/acsami.6b06825.

(40) Xu, T.; Miszuk, J. M.; Zhao, Y.; Sun, H.; Fong, H. Electrospun polycaprolactone 3D nanofibrous scaffold with interconnected and hierarchically structured pores for bone tissue engineering. *Adv Healthc Mater* **2015,** *4* (15), 2238-46, DOI: 10.1002/adhm.201500345.

(41) Girao, A. F.; Goncalves, G.; Bhangra, K. S.; Phillips, J. B.; Knowles, J.; Irurueta, G.; Singh, M. K.; Bdkin, I.; Completo, A.; Marques, P. A. A. P. Electrostatic self-assembled graphene oxide-collagen scaffolds towards a three-dimensional microenvironment for biomimetic applications. *RSC Adv.* **2016,** *6* (54), 49039-49051, DOI: 10.1039/c6ra10213a.

(42) Mondal, D.; Griffith, M.; Venkatraman, S. S. Polycaprolactone-based biomaterials for tissue engineering and drug delivery: Current scenario and challenges. *Int J Polym Mater* **2016,** *65* (5), 255-265, DOI: 10.1080/00914037.2015.1103241.

(43) Glowacki, J.; Mizuno, S. Collagen scaffolds for tissue engineering. *Biopolymers* **2008,** *89* (5), 338-344, DOI: 10.1002/bip.20871.

(44) Elzein, T.; Nasser-Eddine, M.; Delaite, C.; Bistac, S.; Dumas, P. FTIR study of polycaprolactone chain organization at interfaces. *J. Colloid Interface Sci.* **2004,** *273* (2), 381-387, DOI: https://doi.org/10.1016/j.jcis.2004.02.001.

(45) Naseri, N.; Poirier, J.-M.; Girandon, L.; Frohlich, M.; Oksman, K.; Mathew, A. P. 3-Dimensional porous nanocomposite scaffolds based on cellulose nanofibers for cartilage tissue engineering: tailoring of porosity and mechanical performance. *RSC Adv.* **2016,** *6* (8), 5999-6007, DOI: 10.1039/c5ra27246g.

(46) Kostakova, E.; Seps, M.; Pokorny, P.; Lukas, D. Study of polycaprolactone wet electrospinning process. *Express Polym Lett* **2014,** *8* (8), 554-564, DOI: 10.3144/expresspolymlett.2014.59.

(47) Yokoyama, Y.; Hattori, S.; Yoshikawa, C.; Yasuda, Y.; Koyama, H.; Takato, T.; Kobayashi, H. Novel wet electrospinning system for fabrication of spongiform nanofiber 3-dimensional fabric. *Mater. Lett.* **2009,** *63* (9), 754-756, DOI: https://doi.org/10.1016/j.matlet.2008.12.042.

(48) Ki, C. S.; Kim, J. W.; Hyun, J. H.; Lee, K. H.; Hattori, M.; Rah, D. K.; Park, Y. H. Electrospun three-dimensional silk fibroin nanofibrous scaffold. *J. Appl. Polym. Sci.* **2007,** *106* (6), 3922-3928, DOI: 10.1002/app.26914.

(49) Kim, M. S.; Kim, G. H. Highly porous electrospun 3D polycaprolactone/β-TCP biocomposites for tissue regeneration. *Mater. Lett.* **2014,** *120*, 246-250, DOI: https://doi.org/10.1016/j.matlet.2014.01.083.

(50) Yang, W.; Yang, F.; Wang, Y.; Both, S. K.; Jansen, J. A. In vivo bone generation via the endochondral pathway on three-dimensional electrospun fibers. *Acta Biomater.* **2013,** *9* (1), 4505-4512, DOI: https://doi.org/10.1016/j.actbio.2012.10.003.

(51) Zhang, X.; Chang, W.; Lee, P.; Wang, Y.; Yang, M.; Li, J.; Kumbar, S. G.; Yu, X. Polymer-Ceramic Spiral Structured Scaffolds for Bone Tissue Engineering: Effect of Hydroxyapatite Composition on Human Fetal Osteoblasts. *PLOS ONE* **2014,** *9* (1), e85871, DOI: 10.1371/journal.pone.0085871.

(52) Deng, M.; Kumbar, S. G.; Nair, L. S.; Weikel, A. L.; Allcock, H. R.; Laurencin, C. T. Biomimetic Structures: Biological Implications of Dipeptide-Substituted Polyphosphazene–Polyester Blend Nanofiber Matrices for Load-Bearing Bone Regeneration. *Adv. Funct. Mater.* **2011,** *21* (14), 2641-2651, DOI: 10.1002/adfm.201100275.

(53) Kutikov, A. B.; Skelly, J. D.; Ayers, D. C.; Song, J. Templated repair of long bone defects in rats with bioactive spiral-wrapped electrospun amphiphilic polymer/hydroxyapatite scaffolds. *ACS Appl Mater Interfaces* **2015,** *7* (8), 4890-901, DOI: 10.1021/am508984y.

(54) Piskin, E.; Isoglu, I. A.; Bolgen, N.; Vargel, I.; Griffiths, S.; Cavusoglu, T.; Korkusuz, P.; Guzel, E.; Cartmell, S. In vivo performance of simvastatin-loaded electrospun spiral-wound polycaprolactone scaffolds in reconstruction of cranial bone defects in the rat model. *J Biomed Mater Res A* **2009,** *90* (4), 1137-51, DOI: 10.1002/jbm.a.32157.

(55) Wang, J.; Valmikinathan, C. M.; Liu, W.; Laurencin, C. T.; Yu, X. Spiral-structured, nanofibrous, 3D scaffolds for bone tissue engineering. *J Biomed Mater Res A* **2010,** *93* (2), 753-62, DOI: 10.1002/jbm.a.32591.

(56) Hejazi, F.; Mirzadeh, H. Roll-designed 3D nanofibrous scaffold suitable for the regeneration of load bearing bone defects. *Prog Biomater.* **2016,** *5* (3), 199-211, DOI: 10.1007/s40204-016-0058-2.

(57) Eckstein, F.; Lemberger, B.; Gratzke, C.; Hudelmaier, M.; Glaser, C.; Englmeier, K. H.; Reiser, M. In vivo cartilage deformation after different types of activity and its dependence on physical training status. *Ann. Rheum. Dis.* **2005,** *64* (2), 291.

(58) Kim, O. V.; Liang, X.; Litvinov, R. I.; Weisel, J. W.; Alber, M. S.; Purohit, P. K. Foam-like compression behavior of fibrin networks. *Biomech Model Mechanobiol* **2016,** *15* (1), 213-228, DOI: 10.1007/s10237-015-0683-z.

(59) Maiolo, A. S.; Amado, M. N.; Gonzalez, J. S.; Alvarez, V. A. Development and characterization of Poly (vinyl alcohol) based hydrogels for potential use as an articular cartilage replacement. *Materials Science and Engineering: C* **2012,** *32* (6), 1490-1495, DOI: https://doi.org/10.1016/j.msec.2012.04.030.

(60) Schuh, E.; Kramer, J.; Rohwedel, J.; Notbohm, H.; Muller, R.; Gutsmann, T.; Rotter, N. Effect of matrix elasticity on the maintenance of the chondrogenic phenotype. *Tissue Eng Part A* **2010,** *16* (4), 1281-90, DOI: 10.1089/ten.TEA.2009.0614.

(61) McLeod, M. A.; Wilusz, R. E.; Guilak, F. Depth-Dependent Anisotropy of the Micromechanical Properties of the Extracellular and Pericellular Matrices of Articular Cartilage

Evaluated via Atomic Force Microscopy. *J. Biomech.* **2013,** *46* (3), 586-592, DOI: 10.1016/j.jbiomech.2012.09.003.

(62) Fahy, N.; Alini, M.; Stoddart, M. J. Mechanical stimulation of mesenchymal stem cells: Implications for cartilage tissue engineering. *J Orthop Res* **2017**, DOI: 10.1002/jor.23670.

(63) Meinert, C.; Schrobback, K.; Hutmacher, D. W.; Klein, T. J. A novel bioreactor system for biaxial mechanical loading enhances the properties of tissue-engineered human cartilage. *Scientific Reports* **2017,** *7* (1), 16997, DOI: 10.1038/s41598-017-16523-x.

(64) Schulz, R. M.; Bader, A. Cartilage tissue engineering and bioreactor systems for the cultivation and stimulation of chondrocytes. *Eur Biophys J* **2007,** *36* (4-5), 539-68, DOI: 10.1007/s00249-007-0139-1.

(65) Completo, A.; Mendes, A. Bioreactor de estímulo para caracterização biomecânica de engenharia de tecidos. PATENTE DE INVENÇÃO NACIONAL Nº 106827. 2013.

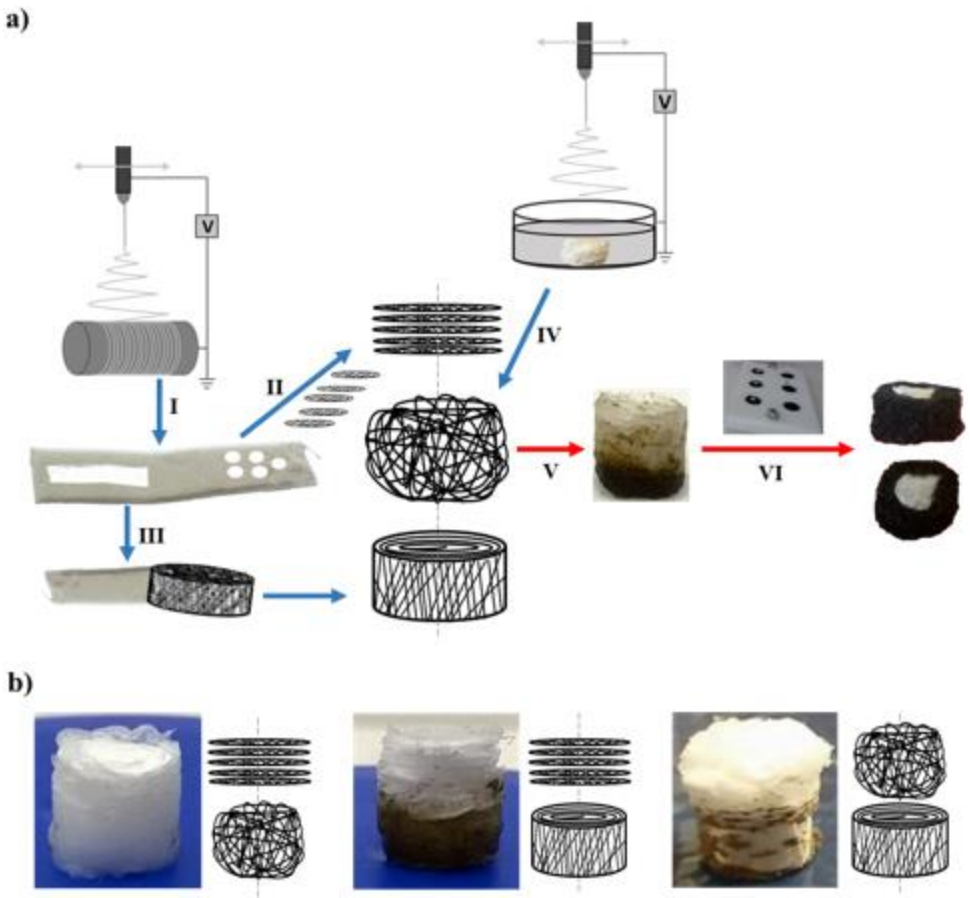

Figure 1. Schematic of the fabrication of the PCL-GO-collagen scaffold. **a)** fabrication process: I – electrospinning onto a rotating drum; II – cutting cylinders from the electrospun mesh for building the superficial layer; III – rolling a small rectangle from the electrospun mesh within the GO-collagen hydrogel; IV – electrospinning onto an ethanol:water bath for producing the middle layer; V – assembling and freezing the layers in order to fabricate a three-layered electrospun scaffold; VI – incorporating the anisotropic 3D electrospun structure within the GO-collagen hydrogel with the purpose of creating a microporous network able to support and involve the electrospun structure after freeze-drying; **b)** alternative geometric architectures used during the assembly process: from the right to left – geometry 2 (superficial + middle layers); geometry 3 (superficial + deep layers) and geometry 4 (middle + deep layers).

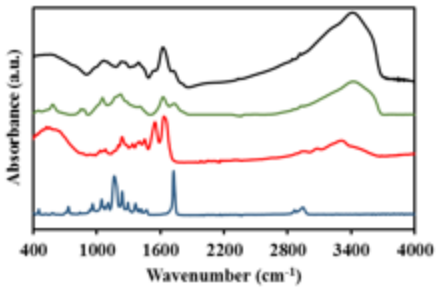

Figure 2. Chemical characterization of the materials used. ATR-FTIR spectra of PCL (blue), collagen (red), GO (green) and GO-collagen composite (black).

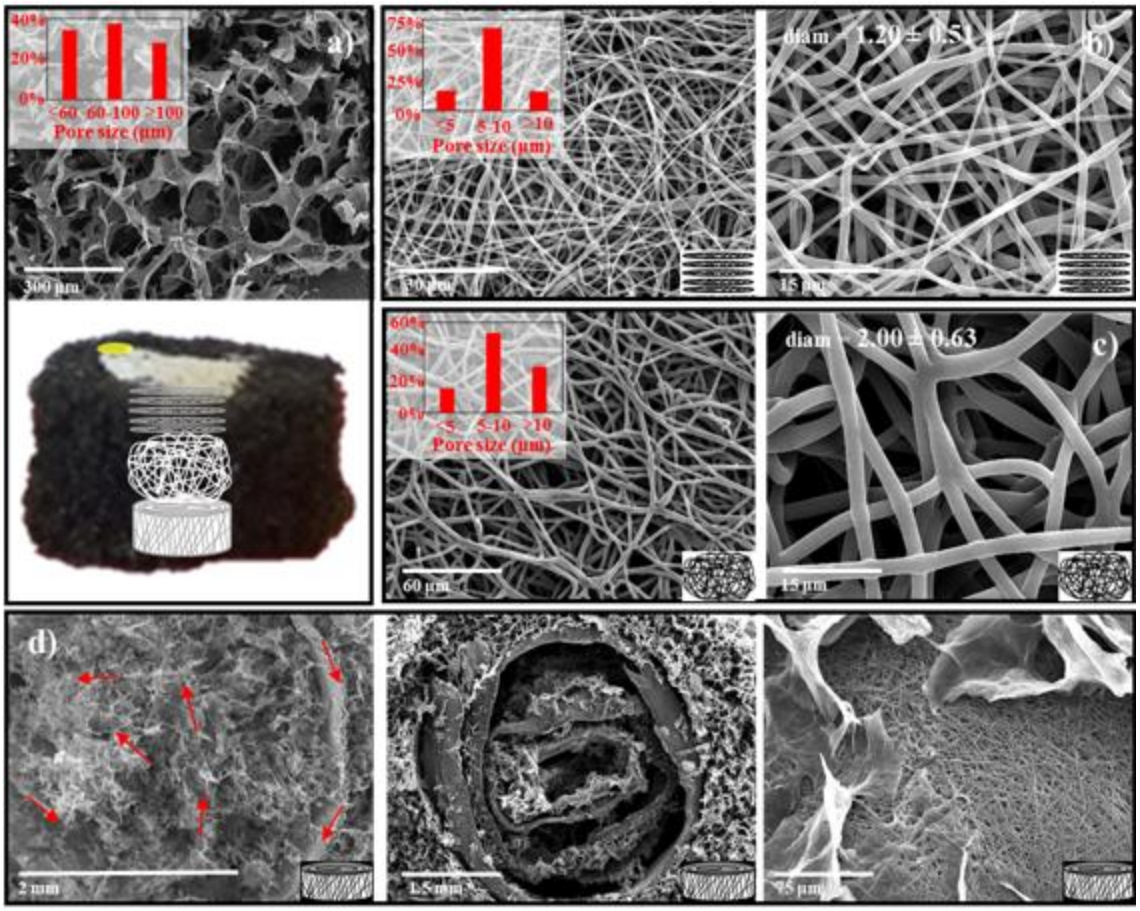

Figure 3. PCL-GO-collagen (geometry 1) morphological characterization. **a)** PCL-GO-collagen scaffold with geometry 1 with a tri-layered anisotropic fibrous scheme (down) and the microporous GO-collagen that surrounds it (up -magnification of the yellow area); **b)** Superficial layer; **c)** Middle layer; **d)** Deep layer: left - 3D fibrous spiral (red arrows) with its branches intercalated with GO-collagen porous network, middle – 3D fibrous spiral with the GO-collagen porous network removed, right – boundary between the GO-collagen network and the PCL fibers.

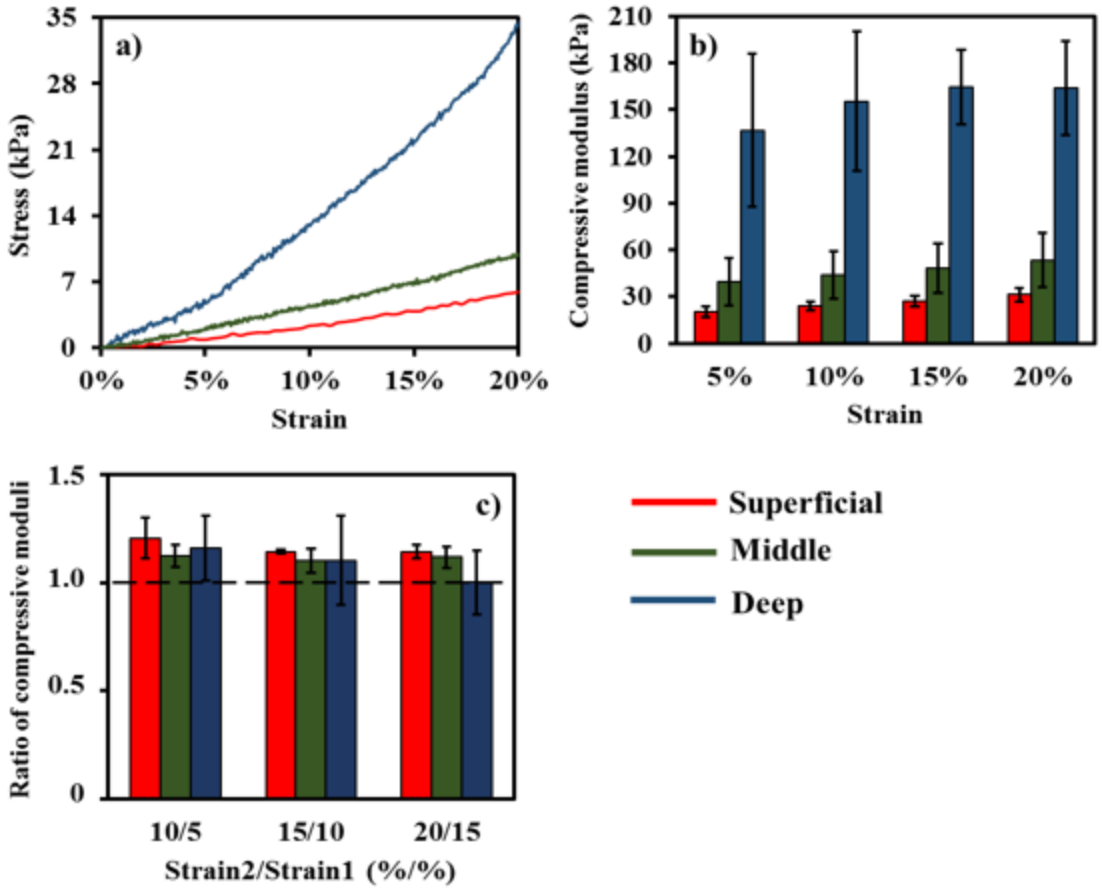

Figure 4. Compressive properties of the electrospun layers. **a)** Stress strain curves; **b)** compressive moduli for 5%, 10%, 15% and 20% strain values; **c)** ratio of the compressive moduli.

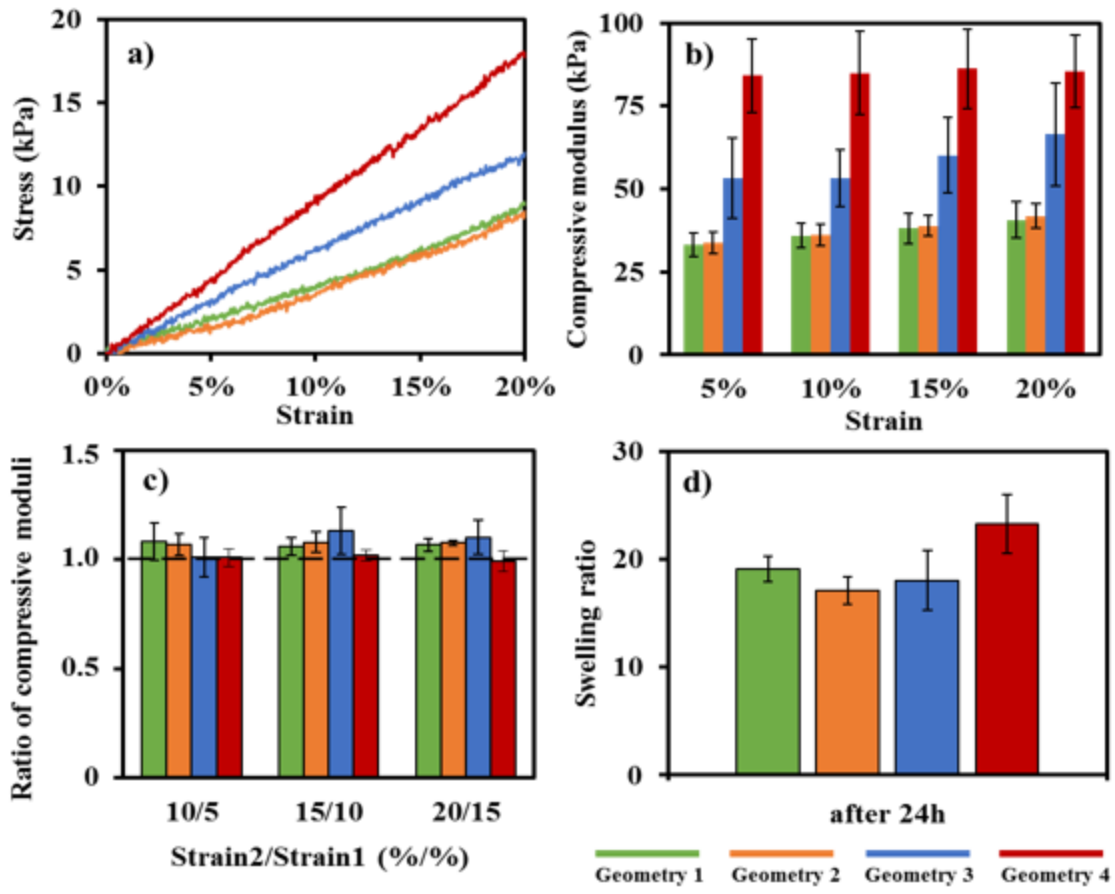

Figure 5. Compressive properties of the anisotropic PCL-GO-collagen scaffolds. **a)** Stress-strain curves; **b)** compressive moduli for 5%, 10%, 15% and 20% strain values; **c)** ratio of compressive moduli; **d)** swelling ratio after 24h.

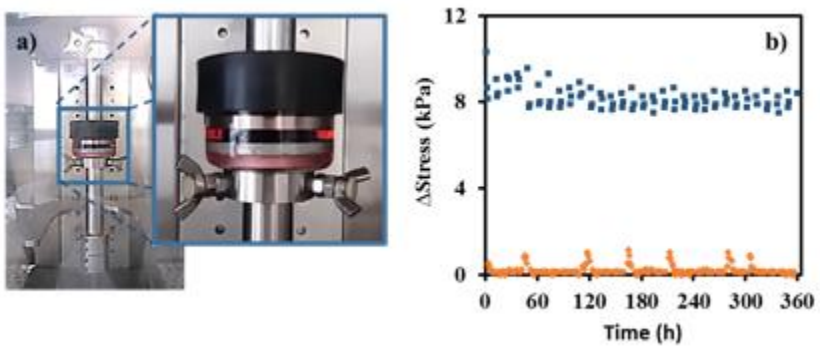

Figure 6. Dynamic compression of the PCL-GO-collagen scaffolds. **a)** Bioreactor apparatus with an amplification of the chamber where the PCL-GO-collagen scaffolds are placed during mechanical stimulation; **b)** Mechanical response of the PCL-GO-collagen scaffolds under dynamic compression cycles - Blue: Stimulation. Orange: Rest. The slightly variations in the rest periods corresponded to the time points when the cell medium was changed.

Table 1. Compressive properties of the electrospun layers.

Property	Strain	Electrospun layers		
		Superficial	Middle	Deep
Compressive Modulus (kPa)	5%	19.99 ± 3.40	39.52 ± 15.34	136.77 ± 49.30
	10%	23.92 ± 3.00	43.92 ± 15.28	155.39 ± 44.78
	15%	27.33 ± 3.42	48.09 ± 15.99	164.46 ± 24.11
	20%	31.28 ± 4.00	53.48 ± 17.22	164.15 ± 30.13
Ratio of Compressive moduli	10% / 5%	1.21 ± 0.09	1.12 ± 0.05	1.16 ± 0.15
	15% / 10%	1.14 ± 0.01	1.10 ± 0.06	1.10 ± 0.21
	20% / 15%	1.14 ± 0.03	1.12 ± 0.05	1.00 ± 0.15

Table 2. Compressive and swelling properties of the PCL-GO-collagen scaffolds.

Property	Strain	PCL-GO-collagen scaffolds			
		Geometry 1	Geometry 2	Geometry 3	Geometry 4
Compressive Modulus (kPa)	5%	33.24 ± 3.58	33.77 ± 3.14	53.38 ± 12.09	84.14 ± 11.10
	10%	35.90 ± 3.74	36.09 ± 3.19	53.24 ± 8.57	84.94 ± 12.58
	15%	38.07 ± 4.48	38.90 ± 3.06	60.12 ± 11.31	86.27 ± 11.94
	20%	40.69 ± 5.48	41.86 ± 3.57	66.47 ± 15.49	85.42 ± 10.91
Ratio of Compressive moduli	10% / 5%	1.08 ± 0.08	1.07 ± 0.05	1.01 ± 0.09	1.01 ± 0.04
	15% / 10%	1.06 ± 0.04	1.08 ± 0.05	1.13 ± 0.11	1.02 ± 0.02
	20% / 15%	1.07 ± 0.03	1.08 ± 0.01	1.10 ± 0.08	0.99 ± 0.05
Swelling Ratio (24 h)		19.08 ± 1.14	17.11 ± 1.25	18.03 ± 2.75	23.22 ± 2.71

Graphical Abstract